

Pion-nucleon scattering to order p^4 in SU(3) heavy baryon chiral perturbation theory

Bo-Lin Huang ^{*1}

¹Department of Physics, Jishou University, Jishou 416000, China

January 19, 2022

Abstract

We calculate the T -matrices of elastic pion-nucleon (πN) scattering up to fourth order in SU(3) heavy baryon chiral perturbation theory. The baryon mass in the chiral limit M_0 and the pertinent low-energy constants are determined by fitting to empirical πN phase shifts below 200 MeV pion laboratory momentum in the physical region. The scattering lengths and scattering volumes are also extracted from the chiral amplitudes, and turn out to be in good agreement with those of other approaches and the available experimental values. On the basis of the various phase shifts and the threshold parameters, the convergence of the chiral expansion is analyzed in detail. A good convergence for πN scattering observables is obtained when working up to fourth order. In addition, we extend the fit to 250 MeV pion laboratory momentum, and obtain also a good description of the empirical S - and P -wave phase shifts.

PACS numbers: 13.75.Jz,12.39.Fe,12.38.Bx

Keywords: Chiral perturbation theory, pion-nucleon scattering, chiral convergence

1 Introduction

Chiral perturbation theory (ChPT) allows one to analyze hadronic processes at low energies, that are not accessible by a perturbative expansion in the strong coupling constant α_s of quantum chromodynamics (QCD)[1, 2, 3, 4]. ChPT is an efficient framework to calculate in a model-independent way e.g. the amplitudes of pion-nucleon (πN) scattering below the chiral symmetry breaking scale $\Lambda_\chi \simeq 1\text{GeV}$. However, there exists a power-counting problem in baryon ChPT because of the non-vanishing baryon mass M_0 in the chiral limit. Over the years, several approaches have been proposed to solve this problem. Heavy baryon ChPT (HB χ PT) [5, 6], the infrared regularization of covariant baryon ChPT [7], and the extended-on-mass-shell scheme for baryon ChPT [8, 9] are some popular approaches. The last two approaches are fully relativistic and have lead to substantial progress in many aspects as documented in ref. [10, 11, 12, 13, 14, 15, 16]. However, the expressions from the loop diagrams become rather complicated in these fully relativistic approaches [17, 18, 19]. On the other hand, HB χ PT is a well-established and versatile tool for the study of low-energy hadronic processes. The amplitudes in HB χ PT proceeds simultaneously in terms of p/Λ_χ (non-relativistic contributions from tree- and loop-diagrams) and p/M_0 (relativistic corrections), where p denotes the meson momentum (or mass) or the small residual momentum of a baryon in a low-energy process.

In recent years, there has been renewed interest in theoretical studies of elastic meson-baryon scattering at low energies. These are not only concerned with the description of the strong mesonic interaction, but also with the chiral properties of the baryons. The low-energy processes between pions and nucleons have been investigated extensively in SU(2) HB χ PT in refs. [20, 21, 22, 23]. Furthermore, the subthreshold parameters of pion-nucleon scattering have also been deeply studied by combined with Roy-Steiner equations and SU(2) ChPT [24, 25]. For processes involving kaons or hyperons, the situation becomes more involved, since one has to work out the consequences of three-flavor chiral dynamics. In a previous paper [26] we have investigated KN and $\bar{K}N$ elastic scattering up to one-loop order in SU(3) HB χ PT by fitting low-energy

*bolin.huang@foxmail.com

constants to partial-wave phase shifts of KN -scattering and obtained quite reasonable results. This approach was then extended by predicting the amplitudes of pseudoscalar-meson octet-baryon scattering in all channels, with the pertinent low-energy constants fitted to partial-wave phase shifts of elastic πN and KN scattering [27]. At this point one should note that the detailed predictions of SU(3) HB χ PT for the meson-baryon scattering lengths have been given previously in refs. [28, 29, 30, 31, 32]. Moreover, these studies in SU(3) HB χ PT has been extended to partial-wave phase shifts, the pion-nucleon sigma term, and other quantities. In a recent paper [33], we have calculated the complete T -matrices of pion-nucleon scattering up to third order in SU(3) HB χ PT and obtained as a byproduct nucleon properties, like the pion-nucleon sigma term $\sigma_{\pi N}$. A good description of the phase shifts of πN scattering below 200 MeV has been obtained, and then it can serve as a consistency check to consider also the other meson-baryon scattering channels. However, no good convergence of the chiral expansion is observed in calculations that terminate at third order. Therefore, we will compute in this paper the T -matrices for πN scattering up to fourth order in SU(3) HB χ PT. The parameter M_0 and the pertinent low-energy constants (LECs) will be determined by fitting to empirical S - and P -wave phase shifts of πN scattering. In particular, the LECs related to contact terms of chiral dimension will be obtained separately. The convergence of the chiral expansions will be analyzed and discussed in detail. Since chiral expansions should become more accurate by increasing the chiral order, the description of the empirical πN phase shifts at somewhat higher energies will also be presented.

The present paper is organized as follows. In Sec. 2, we summarize the Lagrangians involved in the evaluation of the fourth-order contributions. In Sec. 3, we present some explicit expressions for the T -matrices of elastic πN scattering at order p^4 . In Sec. 4, we outline how to derive phase shifts, scattering lengths, and scattering volumes from the T -matrices. Section 5 contains the presentation and discussion of our results and it also includes a brief summary.

2 Chiral Lagrangian

In order to calculate the pion-nucleon scattering amplitude up to order p^4 in SU(3) heavy baryon chiral perturbation theory, one has to evaluate tree- and loop diagrams with vertices from the effective chiral Lagrangian:

$$\mathcal{L}_{\text{eff}} = \mathcal{L}_{\phi\phi}^{(2)} + \mathcal{L}_{\phi B}^{(1)} + \mathcal{L}_{\phi B}^{(2)} + \mathcal{L}_{\phi B}^{(3)} + \mathcal{L}_{\phi B}^{(4)}. \quad (1)$$

These Lagrangians are written in terms of the traceless hermitian 3×3 matrices ϕ and B that include the pseudoscalar Goldstone boson fields (π , K , \bar{K} , η) and the octet-baryon fields (N , Λ , Σ , Ξ), respectively. The explicit form of the $\mathcal{L}_{\phi\phi}^{(2)}$, $\mathcal{L}_{\phi B}^{(1)}$, $\mathcal{L}_{\phi B}^{(2)}$ and $\mathcal{L}_{\phi B}^{(3)}$ can be found in ref. [33]. The complete fourth-order heavy baryon Lagrangian $\mathcal{L}_{\phi B}^{(4)}$ naturally splits up into two parts: relativistic corrections with fixed coefficients, and counterterms proportional to new low-energy constants. The relativistic terms can be obtained from the original leading-order, next-to-leading-order and next-to-next-to-leading-order lorentz-invariant Lagrangians through path integral manipulations [6]. For three-flavors and at chiral order four, the lorentz-invariant meson-baryon Lagrangian has been constructed in ref. [34] and we can obtain from it the counterterms relevant for our purpose. Since the dimension-four chiral meson-baryon Lagrangian $\mathcal{L}_{\phi B}^{(4)}$ is very lengthy, the explicit expressions will not be given in this paper, where we consider only elastic pion-nucleon scattering. Of course, the expansions in SU(3) and SU(2) HB χ PT are consistent with each other. For this reason the notation of low-energy constants \bar{e}_i ($i = 14, \dots, 22, 35, \dots, 38$) for the fourth-order counterterms in SU(2) HB χ PT introduced in ref. [21] will also be used in this paper.

3 T -matrices for pion-nucleon scattering

We are considering the elastic pion-nucleon scattering process $\pi(q) + N(p) \rightarrow \pi(q') + N(p')$ in the center-of-mass system (cms). In states with total isospin $I = 1/2$ or $I = 3/2$ of the pion-nucleon system, the corresponding T -matrix takes the following form in spin-space:

$$T_{\pi N}^{(I)} = V_{\pi N}^{(I)}(w, t) + i\boldsymbol{\sigma} \cdot (\mathbf{q}' \times \mathbf{q}) W_{\pi N}^{(I)}(w, t) \quad (2)$$

where $w = q_0 = q'_0 = (m_\pi^2 + \mathbf{q}^2)^{1/2}$ is the pion cms-energy, and $t = (q' - q)^2 = 2\mathbf{q}^2(z - 1)$ is the invariant momentum-transfer squared with $z = \cos\theta$ the cosine of the angle θ between \mathbf{q} and \mathbf{q}' .

Based on relativistic kinematics, one gets the relation:

$$\mathbf{q}'^2 = \mathbf{q}^2 = \frac{M_N^2 \mathbf{p}_{\text{lab}}^2}{m_\pi^2 + M_N^2 + 2M_N \sqrt{m_\pi^2 + \mathbf{p}_{\text{lab}}^2}}, \quad (3)$$

where \mathbf{p}_{lab} denotes the momentum of the incident meson in the laboratory system. Furthermore, $V_{\pi N}^{(I)}(w, t)$ refers to the non-spin-flip pion-nucleon scattering amplitude and $W_{\pi N}^{(I)}(w, t)$ is called the spin-flip pion-nucleon scattering amplitude.

From leading order $\mathcal{O}(p)$ up to third order $\mathcal{O}(p^3)$, the expressions for the amplitudes $V_{\pi N}^{(I)}(w, t)$ and $W_{\pi N}^{(I)}(w, t)$ can be found in ref. [33]. At fourth order $\mathcal{O}(p^4)$, the SU(3) results for the πN amplitudes from tree diagrams are essentially the same as those calculated in SU(2) HB χ PT in ref. [21]. After an appropriate renaming of the low-energy constants, these contributions read:

$$\begin{aligned} V_{\pi N}^{(3/2, \text{N3LO})} = & -\frac{(D+F)^2}{32M_0^3 w^4 f_\pi^2} [(t^4 + 7t^3 w^2 + 11t^2 w^4 - 3tw^6 + 4w^8) - (11t^3 + 49t^2 w^2 + 32tw^4 \\ & + 4w^6)m_\pi^2 + (45t^2 + 110tw^2 + 26w^4)m_\pi^4 - 3(27t + 26w^2)m_\pi^6 + 54m_\pi^8] \\ & + \frac{m_\pi^2 - w^2}{32M_0^3 f_\pi^2} (4m_\pi^2 - t - 4w^2) + \frac{1}{16M_0^2 f_\pi^2} [4C_0(t + 2w^2 - 2m_\pi^2)m_\pi^2 + C_1(2t^2 + 4tw^2 \\ & - 8tm_\pi^2 - 8w^2 m_\pi^2 + 8m_\pi^4) + 4C_2(3tw^2 + 14w^4 - 4tm_\pi^2 - 22w^2 m_\pi^2 + 8m_\pi^4) \\ & + 2C_3(-t^2 - 4tw^2 + 4tm_\pi^2)] - \frac{8}{M_0 f_\pi^2} C_0 C_2 w^2 m_\pi^2 + \frac{1}{2M_0 f_\pi^2} [H_1(4m_\pi^2 - t - 4w^2)m_\pi^2 \\ & + H_2(4w^2 + t - 4m_\pi^2)t + 3H_3(4m_\pi^2 - t - 4w^2)w^2 + 2H_4 w^2 t] \\ & + \frac{1}{f_\pi^2} [4\bar{e}_{14}(4m_\pi^4 - 4m_\pi^2 t - t^2) + 8\bar{e}_{15}(2w^2 m_\pi^2 - tw^2) + 16\bar{e}_{16} w^4], \end{aligned} \quad (4)$$

$$\begin{aligned} W_{\pi N}^{(3/2, \text{N3LO})} = & \frac{(D+F)^2}{16M_0^3 w^4 f_\pi^2} [(t^3 + 5t^2 w^2 + 3tw^4 - w^6) - (9t^2 + 25tw^2 + 4w^4)m_\pi^2 \\ & + 3(9t + 10w^2)m_\pi^4 - 27m_\pi^6] + \frac{w^2 - m_\pi^2}{16M_0^3 f_\pi^2} + \frac{1}{8M_0^2 f_\pi^2} [8C_0 m_\pi^2 + C_1(2t - 4m_\pi^2) \\ & - 4C_2 w^2 - 2C_3(t + 2w^2 - 2m_\pi^2)] + \frac{1}{2M_0 f_\pi^2} H_4(8w^2 + t - 4m_\pi^2) \\ & + \frac{1}{f_\pi^2} [\bar{e}_{17}(-8m_\pi^2 + 4t) - 8\bar{e}_{18} w^2], \end{aligned} \quad (5)$$

$$\begin{aligned} V_{\pi N}^{(1/2, \text{N3LO})} = & \frac{(D+F)^2}{64M_0^3 w^4 f_\pi^2} [(t^4 + 7t^3 w^2 + 11t^2 w^4 + 16w^8) - (11t^3 + 49t^2 w^2 + 32tw^4 \\ & + 16w^6)m_\pi^2 + 5(9t^2 + 22tw^2 + 4w^4)m_\pi^4 - 84(t + w^2)m_\pi^6 + 60m_\pi^8] \\ & + \frac{w^2 - m_\pi^2}{16M_0^3 f_\pi^2} (4m_\pi^2 - t - 4w^2) + \frac{1}{8M_0^2 f_\pi^2} [2C_0(t + 2w^2 - 2m_\pi^2)m_\pi^2 + C_1(t^2 + 2tw^2 \\ & - 4tm_\pi^2 - 4w^2 m_\pi^2 + 4m_\pi^4) + 2C_2(3tw^2 + 14w^4 - 4tm_\pi^2 - 22w^2 m_\pi^2 + 8m_\pi^4) \\ & + 2C_3(t^2 + 4tw^2 - 4tm_\pi^2)] - \frac{8}{M_0 f_\pi^2} C_0 C_2 w^2 m_\pi^2 + \frac{1}{M_0 f_\pi^2} [H_1(-4m_\pi^2 + t + 4w^2)m_\pi^2 \\ & - H_2(4w^2 + t - 4m_\pi^2)t - 3H_3(4m_\pi^2 - t - 4w^2)w^2 + H_4 w^2 t] \\ & + \frac{1}{f_\pi^2} [4\bar{e}_{14}(4m_\pi^4 - 4m_\pi^2 t - t^2) + 8\bar{e}_{15}(2w^2 m_\pi^2 - tw^2) + 16\bar{e}_{16} w^4], \end{aligned} \quad (6)$$

$$\begin{aligned} W_{\pi N}^{(1/2, \text{N3LO})} = & \frac{(D+F)^2}{32M_0^3 w^4 f_\pi^2} [(-t^3 - 5t^2 w^2 - 3tw^4 + 4w^6) + (9t^2 + 25tw^2 + 4w^4)m_\pi^2 \\ & - 3(9t + 10w^2)m_\pi^4 + 24m_\pi^6] + \frac{m_\pi^2 - w^2}{8M_0^3 f_\pi^2} + \frac{1}{4M_0^2 f_\pi^2} [-2C_0 m_\pi^2 + C_1(t - 2m_\pi^2) - 2C_2 w^2 \\ & + 2C_3(t + 2w^2 - 2m_\pi^2)] + \frac{H_4}{2M_0 f_\pi^2} (8w^2 + t - 4m_\pi^2) + \frac{8}{f_\pi^2} [\bar{e}_{17}(2m_\pi^2 - t) + 2\bar{e}_{18} w^2], \end{aligned} \quad (7)$$

where C_i ($i = 0, 1, 2, 3$) and H_i ($i = 1, 2, 3, 4$) are linear combinations of low-energy constants defined in eq.(22) and eq.(27) of ref. [33], respectively. For the dimension-four LECs, we follow the same strategy as in ref. [21]. The subset of dimension-four low-energy constants \bar{e}_i ($i = 19, 20, 21, 22, 35, 36, 37, 38$) can be absorbed onto the dimension-two LECs c_i ($i = 1, 2, 3, 4$), see eq.(3.23) in ref. [21]. We note that, the dimension-two LECs c_i ($i = 1, 2, 3, 4$) introduced in SU(2) HB χ PT can be replaced equivalently by the combinations of LECs C_i ($i = 0, 1, 2, 3$) of SU(3) HB χ PT. Thus, \bar{e}_i ($i = 14, 15, 16, 17, 18$) are the five remaining dimension-four LECs that are relevant in our calculation. At fourth order, additional πN amplitudes from one-loop diagrams must be taken into account. The pertinent one-loop diagrams generated by the interaction vertices from $\mathcal{L}_{\phi\phi}^{(2)}$, $\mathcal{L}_{\phi B}^{(1)}$ and $\mathcal{L}_{\phi B}^{(2)}$ are shown in Figure 1. The expressions for these one-loop πN amplitudes are rather tedious and will therefore not be reproduced here. The explicit analytical expressions for the loop contributions of order $\mathcal{O}(p^4)$ to elastic πN scattering can be obtained from the authors upon request. For orientation of the readers, we remark that these πN loop-amplitudes are composed of the following basic loop-functions:

$$J_0(w, m) = \frac{1}{i} \int \frac{d^D l}{(2\pi)^D} \frac{1}{(v \cdot l - w)(m^2 - l^2)} = \frac{w}{8\pi^2} \left(1 - 2\ln \frac{m}{\lambda}\right) + \begin{cases} \frac{1}{4\pi^2} \sqrt{w^2 - m^2} \ln \frac{-w + \sqrt{w^2 - m^2}}{m} & (w < -m), \\ -\frac{1}{4\pi^2} \sqrt{m^2 - w^2} \arccos \frac{-w}{m} & (-m < w < m), \\ \frac{1}{4\pi^2} \sqrt{w^2 - m^2} \left(i\pi - \ln \frac{w + \sqrt{w^2 - m^2}}{m} \right) & (w > m), \end{cases} \quad (8)$$

$$\frac{1}{i} \int \frac{d^D l}{(2\pi)^D} \frac{\{1, l^\mu, l^\mu l^\nu\}}{(m^2 - l^2)[m^2 - (l - k)^2]} = \{I_0(t, m), \frac{k^\mu}{2} I_0(t, m), g^{\mu\nu} I_2(t, m) + k^\mu k^\nu I_3(t, m)\}, \quad (9)$$

$$I_0(t, m) = \frac{1}{8\pi^2} \left\{ \frac{1}{2} - \ln \frac{m}{\lambda} - \sqrt{1 - \frac{4m^2}{t}} \ln \frac{\sqrt{4m^2 - t} + \sqrt{-t}}{2m} \right\}, \quad (10)$$

$$I_2(t, m) = \frac{1}{48\pi^2} \left\{ 2m^2 - \frac{5t}{12} + \left(\frac{t}{2} - 3m^2 \right) \ln \frac{m}{\lambda} - \frac{(4m^2 - t)^{3/2}}{2\sqrt{-t}} \ln \frac{\sqrt{4m^2 - t} + \sqrt{-t}}{2m} \right\}, \quad (11)$$

$$I_3(t, m) = \frac{1}{24\pi^2} \left\{ \frac{7}{12} - \frac{m^2}{t} - \ln \frac{m}{\lambda} - \left(1 - \frac{m^2}{t} \right) \sqrt{1 - \frac{4m^2}{t}} \ln \frac{\sqrt{4m^2 - t} + \sqrt{-t}}{2m} \right\}. \quad (12)$$

Note that terms proportional to the divergent constant $\lambda^{D-4} [\frac{1}{D-4} + \frac{1}{2}(\gamma_E - 1 - \ln 4\pi)]$ have been dropped. Furthermore, one observes that the one-loop amplitudes of order $\mathcal{O}(p^4)$ involve the full set of dimension-two LECs b_i ($i = D, F, 0, \dots, 11$) and not just the few combinations of LECs C_i ($i = 0, 1, 2, 3$) arising from tree-diagrams.

4 Partial-wave phase shifts and scattering lengths

The partial-wave amplitudes $f_j^{(I)}(\mathbf{q}^2)$, where $j = l \pm 1/2$ refers to the total angular momentum and l to orbital angular momentum, are obtained from the non-spin-flip and spin-flip amplitudes by the following projection formula:

$$f_{l\pm 1/2}^{(I)}(\mathbf{q}^2) = \frac{M_N}{8\pi\sqrt{s}} \int_{-1}^{+1} dz \left\{ V_{\pi N}^{(I)}(w, t) P_l(z) + \mathbf{q}^2 W_{\pi N}^{(I)}(w, t) [P_{l\pm 1}(z) - z P_l(z)] \right\}, \quad (13)$$

where $P_l(z)$ denotes the conventional Legendre polynomial, and $\sqrt{s} = \sqrt{m_\pi^2 + \mathbf{q}^2} + \sqrt{M_N^2 + \mathbf{q}^2}$ is the total center-of-mass energy. For the energy range considered in this paper, the phase shifts $\delta_{l\pm 1/2}^{(I)}$ are calculated as (see also refs. [20, 35])

$$\delta_{l\pm 1/2}^{(I)}(\mathbf{q}^2) = \arctan \left[|\mathbf{q}| \operatorname{Re} f_{l\pm 1/2}^{(I)}(\mathbf{q}^2) \right]. \quad (14)$$

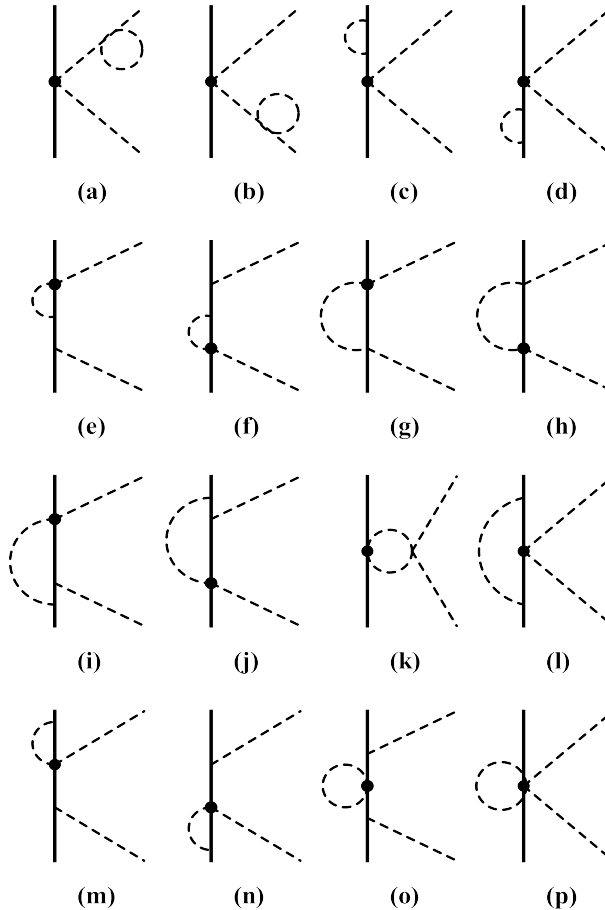


Figure 1: Nonvanishing one-loop diagrams contributing at chiral order four. The heavy dots refer to vertices from $\mathcal{L}_{\phi B}^{(2)}$. Crossed graphs are not shown.

The scattering lengths for S -waves and the scattering volumes for P -waves are obtained by dividing out the threshold behavior of the respective partial-wave amplitude and approaching the threshold [36]

$$a_{l\pm 1/2}^{(I)} = \lim_{|\mathbf{q}| \rightarrow 0} |\mathbf{q}|^{-2l} f_{l\pm 1/2}^{(I)}(\mathbf{q}^2). \quad (15)$$

5 Results and discussion

Before presenting results, we have to determine the M_0 and the LECs. Unfortunately, the 14 dimension-two LECs can not be regrouped up to fourth order in SU(3) HB χ PT. Then, in total, there are 24 unknown constants that need to be determined. Throughout this paper, we also use $m_\pi = 139.57$ MeV, $m_K = 493.68$ MeV, $m_\eta = 547.86$ MeV, $f_\pi = 92.07$ MeV, $f_K = 110.03$ MeV, $f_\eta = 1.2f_\pi$, $M_N = 938.92 \pm 1.29$ MeV, $M_\Sigma = 1191.01 \pm 4.86$ MeV, $M_\Xi = 1318.26 \pm 6.30$ MeV, $M_\Lambda = 1115.68 \pm 5.58$ MeV, $\lambda = 4\pi f_\pi = 1.16$ GeV, $D = 0.80$ and $F = 0.47$ [37, 38, 39].

We have various fitting strategies to determine the pertinent constants, and the related discussion is given in Ref. [33]. One of them is using the octet-baryon masses ($M_{N,\Sigma,\Xi,\Lambda}$) and the phase shifts of πN scattering simultaneously. This can no longer be done up to fourth order due to the appearance of the more constants for octet-baryon masses. Thus, we determine the M_0 and LECs by using the phase shifts of the WI08 solution [40, 41] for πN scattering directly. We choose a common uncertainty of $\pm 2\%$ to all phase shifts before the fitting procedure. The data points of the S and P waves in the range of 50-150 MeV pion lab. momentum are used. Therefore, there are 66 data in total for this fitting. The resulting M_0 and LECs can be found in Fit 1 of Table 1. The uncertainty for the respective parameter is purely estimated (for a detailed discussion, see, e.g., Refs.[42, 43]). It is not surprising that most of LECs are natural size, i.e. the absolute values of these LECs are between one and ten when one introduces the dimensionless

LECs (e.g., $b'_i = 2M_0b_i$), whereas some of LECs come out fairly large. The situation also can be found in SU(2) HB χ PT [21]. We can also find that the baryon mass in the chiral limit M_0 appears small. It is smaller than any physical value of the octet-baryon mass. However, the M_0 value is reasonable because it is a non-physical quantity. The corresponding S - and P -wave phase shifts are shown by the solid lines of Fig. 2. Obviously, we obtain an excellent description of all waves. Especially, the description of the $P33$ -, and $P13$ -wave phase shifts are improved at high energies as compared to the third-order calculation. For comparison, we present results from the best fits up to third (fit 2) and second (fit 3) order in Table 1. Clearly, the resulting M_0 and LECs have different values in the respective order. Thus, for the amplitudes up to the

Table 1: Values of the various fits. The fit 1, 2, 3 refer to the best fit up to fourth, third and second order, respectively. For a detailed description of these fits, see the main text. Note that the (*) values are calculated by b_i .

	Fit 1	Fit 2	Fit 3
M_0 (MeV)	370.56 ± 74.11	1530.20 ± 290.87	373.47 ± 27.65
b_D (GeV $^{-1}$)	-0.18 ± 0.03		
b_F (GeV $^{-1}$)	0.96 ± 0.19		
b_0 (GeV $^{-1}$)	-1.47 ± 0.29		
b_1 (GeV $^{-1}$)	-0.31 ± 0.06		
b_2 (GeV $^{-1}$)	0.12 ± 0.02		
b_3 (GeV $^{-1}$)	-9.24 ± 0.92		
b_4 (GeV $^{-1}$)	3.95 ± 0.39		
b_5 (GeV $^{-1}$)	-11.12 ± 0.56		
b_6 (GeV $^{-1}$)	0.57 ± 0.11		
b_7 (GeV $^{-1}$)	4.77 ± 0.95		
b_8 (GeV $^{-1}$)	1.35 ± 0.27		
b_9 (GeV $^{-1}$)	-2.14 ± 0.43		
b_{10} (GeV $^{-1}$)	-0.33 ± 0.00		
b_{11} (GeV $^{-1}$)	-5.94 ± 0.59		
C_0 (GeV $^{-1}$)	$-2.14 \pm 0.61^{(*)}$	-3.19 ± 0.23	-2.17 ± 0.82
C_1 (GeV $^{-1}$)	$-6.75 \pm 0.14^{(*)}$	-7.39 ± 0.10	-4.49 ± 0.12
C_2 (GeV $^{-1}$)	$-18.66 \pm 1.84^{(*)}$	4.81 ± 0.22	2.87 ± 0.67
C_3 (GeV $^{-1}$)	$-1.08 \pm 1.98^{(*)}$	1.72 ± 0.04	1.18 ± 0.02
H_1 (GeV $^{-2}$)	31.79 ± 6.36	8.77 ± 0.95	
H_2 (GeV $^{-2}$)	5.25 ± 0.53	5.17 ± 0.16	
H_3 (GeV $^{-2}$)	-8.69 ± 0.43	-10.25 ± 0.71	
H_4 (GeV $^{-2}$)	-15.91 ± 0.79	-8.33 ± 0.31	
\bar{e}_{14} (GeV $^{-3}$)	28.64 ± 1.43		
\bar{e}_{15} (GeV $^{-3}$)	25.22 ± 5.04		
\bar{e}_{16} (GeV $^{-3}$)	4.59 ± 0.92		
\bar{e}_{17} (GeV $^{-3}$)	5.61 ± 1.12		
\bar{e}_{18} (GeV $^{-3}$)	5.61 ± 1.12		
$\chi^2/\text{d.o.f.}$	0.62	1.63	4.12

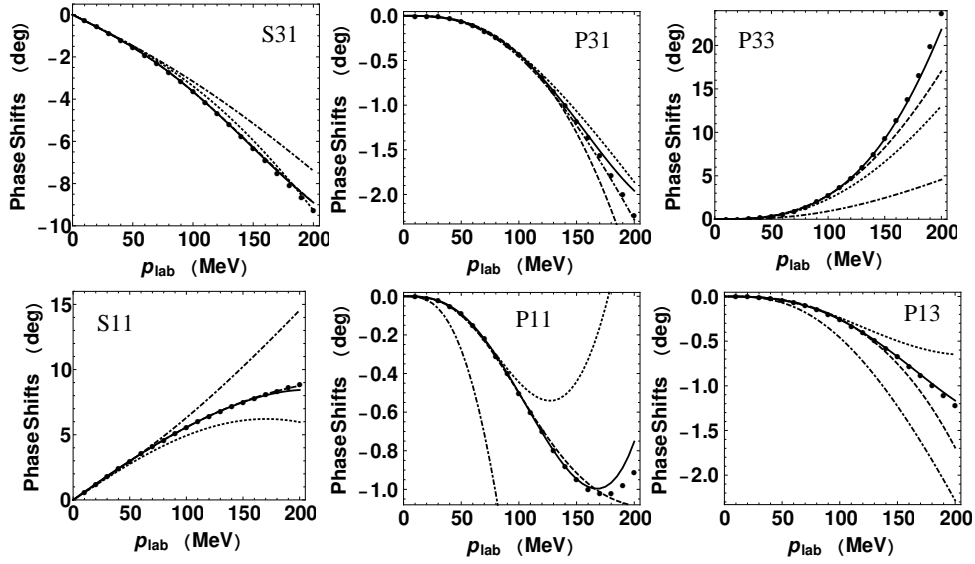


Figure 2: Fits and predictions for the WI08 phase shifts versus the pion lab. momentum $|\mathbf{p}_{\text{lab}}|$ in pion-nucleon (πN) scattering. The dot-dashed, dotted, dashed and solid lines refer to the best fits up to first, second, third and fourth order, respectively. Fitting for all πN waves are the data in the range of 50-150 MeV. For higher and lower energies, the phase shifts are predicted.

given order, the corresponding fit to determine their respective constants is necessary.

In the following, let us apply the chiral fourth order amplitudes to estimate the threshold parameters. Since we do not fit data below 50 MeV, the pion-nucleon scattering lengths and scattering volumes are now predictions. The threshold parameters are obtained by using an incident pion lab. momentum $|\mathbf{p}_{\text{lab}} = 10\text{MeV}|$ and approximating their values at the threshold. The results are shown in Table 2 in comparison with the values of the various analyses. Obviously, our results for both scattering lengths and scattering volumes are consistent with the ones from SU(2) HB χ PT and SP98 [21]. The values of SP98 are obtained by the use of dispersion relations with the help of a fairly precise tree-level model. In addition, there are two experimental values for scattering lengths in Table 2. The values of EXP2001 are from pionic hydrogen and deuterium in ref. [44]. The latter, EXPnew, are obtained by combining with the analysis of the results from refs. [45, 46, 47, 48, 49, 50]. As expected, our results for the threshold parameters are consistent with those values within errors.

Next, we can discuss the convergence of the chiral expansion. In Fig. 2, we show the best fits up to the respective order. In all partial-waves, the fourth-order corrections are smaller than the third-order ones, indicating convergence. In most cases, the third-order corrections are smaller than the second-order ones. The second-order corrections are smaller than the first-order ones in a few partial-waves. Therefore, the convergence of the chiral expansion becomes better along with the increase of the order. However, with the energy increasing the convergence of

Table 2: Values of the S - and P -wave scattering lengths and scattering volumes in comparison with the values of the various analyses.

	Our results	SU(2)	SP98	EXP2001	EXPnew
$a_{0+}^{3/2}$ (fm)	-0.114 ± 0.003	-0.119	-0.125 ± 0.002	-0.125 ± 0.003	-0.119 ± 0.006
$a_{0+}^{1/2}$ (fm)	0.243 ± 0.002	0.249	0.250 ± 0.002	$0.250^{+0.006}_{-0.004}$	0.235 ± 0.002
$a_{1+}^{3/2}$ (fm ³)	0.589 ± 0.021	0.586	0.595 ± 0.005
$a_{1+}^{1/2}$ (fm ³)	-0.072 ± 0.004	-0.054	-0.038 ± 0.008
$a_{1-}^{3/2}$ (fm ³)	-0.108 ± 0.012	-0.113	-0.122 ± 0.006
$a_{1-}^{1/2}$ (fm ³)	-0.171 ± 0.010	-0.181	-0.207 ± 0.007

Table 3: Values of the S - and P -wave scattering lengths and scattering volumes from the different order.

	$\mathcal{O}(q)$	$\mathcal{O}(q^2)$	$\mathcal{O}(q^3)$	$\mathcal{O}(q^4)$
$a_{0+}^{3/2}$ (fm)	-0.113	-0.112 ± 0.067	-0.132 ± 0.042	-0.114 ± 0.003
$a_{0+}^{1/2}$ (fm)	0.225	0.226 ± 0.067	0.214 ± 0.066	0.243 ± 0.002
$a_{1+}^{3/2}$ (fm ³)	0.241	0.569 ± 0.008	0.617 ± 0.014	0.589 ± 0.021
$a_{1+}^{1/2}$ (fm ³)	-0.121	-0.077 ± 0.006	-0.070 ± 0.010	-0.072 ± 0.004
$a_{1-}^{3/2}$ (fm ³)	-0.121	-0.119 ± 0.008	-0.108 ± 0.012	-0.108 ± 0.012
$a_{1-}^{1/2}$ (fm ³)	-0.483	-0.194 ± 0.009	-0.192 ± 0.018	-0.171 ± 0.010

the chiral expansion becomes worse. The fact is not surprising because the chiral expansion is expanded in terms of p/Λ_χ . We can also study the convergence of the threshold parameters, see Table 3. The two scattering lengths $a_{0+}^{3/2}$ and $a_{0+}^{1/2}$ from S waves are almost unchanged in different order, indicating convergence in each order. The other four scattering volumes from P waves are consistent from order $\mathcal{O}(q^2)$. The calculation results indicate the convergence of the threshold parameters is fast that is due to $m_\pi/\Lambda_\chi \sim 1/7$. To sum up, we obtain a good convergence in πN scattering on the basis of the various phase shifts and the threshold parameters.

Inspired by the excellent description of all waves and the good convergence at fourth order, now we extend the fit to 250 MeV pion lab. momentum (corresponding to an energy in CMS of $\sqrt{s} \sim 1.2$ GeV). We also choose a common uncertainty of $\pm 2\%$ to all phase shifts. The data points of the S and P waves in the range of the 50-250 MeV pion lab. momentum are used. Thus, there are 126 data in total for this fitting. The resulting M_0 and LECs are shown in Table 4. We obtain a large $\chi^2/\text{d.o.f.} \simeq 3.15$ because we choose a small common uncertainty to all phase shifts. The value of the baryon mass in the chiral limit M_0 is more close to the physical value and seems more reasonable. The values of the LECs are also different from the values which are obtained by fitting in range of 50-150 MeV pion lab. momentum, see Table 1. The corresponding S - and P -wave phase shifts are shown in Fig. 3. This time, we obtain a good description of all waves except for the $P33$ -wave at high energy. That is due to the existence of the resonance $\Delta(1232)$ in $P33$ -wave. A good description of the $P33$ -wave up to 250 MeV was obtained when the lowest order decuplet contributions were included in Ref. [19]. Thus, for the description of πN phase shifts at high energies, the other hadronic contributions can not be ignored.

In summary, we calculated the T matrices for pion-nucleon scattering to the fourth order in

Table 4: Values of the fit in the range of 50-250MeV at fourth order.

M_0 (MeV)	512.66 ± 102.53	b_9 (GeV ⁻¹)	0.85 ± 0.04
b_D (GeV ⁻¹)	1.80 ± 0.09	b_{10} (GeV ⁻¹)	-1.93 ± 0.08
b_F (GeV ⁻¹)	-1.85 ± 0.09	b_{11} (GeV ⁻¹)	0.45 ± 0.01
b_0 (GeV ⁻¹)	1.46 ± 0.07	H_1 (GeV ⁻²)	46.14 ± 2.31
b_1 (GeV ⁻¹)	-0.92 ± 0.05	H_2 (GeV ⁻²)	10.53 ± 0.53
b_2 (GeV ⁻¹)	-3.00 ± 0.15	H_3 (GeV ⁻²)	-11.22 ± 0.56
b_3 (GeV ⁻¹)	0.06 ± 0.00	H_4 (GeV ⁻²)	-15.65 ± 0.78
b_4 (GeV ⁻¹)	4.05 ± 0.29	\bar{e}_{14} (GeV ⁻³)	6.41 ± 0.33
b_5 (GeV ⁻¹)	-13.04 ± 0.66	\bar{e}_{15} (GeV ⁻³)	-8.42 ± 0.45
b_6 (GeV ⁻¹)	0.23 ± 0.01	\bar{e}_{16} (GeV ⁻³)	8.77 ± 0.44
b_7 (GeV ⁻¹)	8.60 ± 0.45	\bar{e}_{17} (GeV ⁻³)	5.22 ± 0.26
b_8 (GeV ⁻¹)	1.55 ± 0.28	\bar{e}_{18} (GeV ⁻³)	5.22 ± 0.26

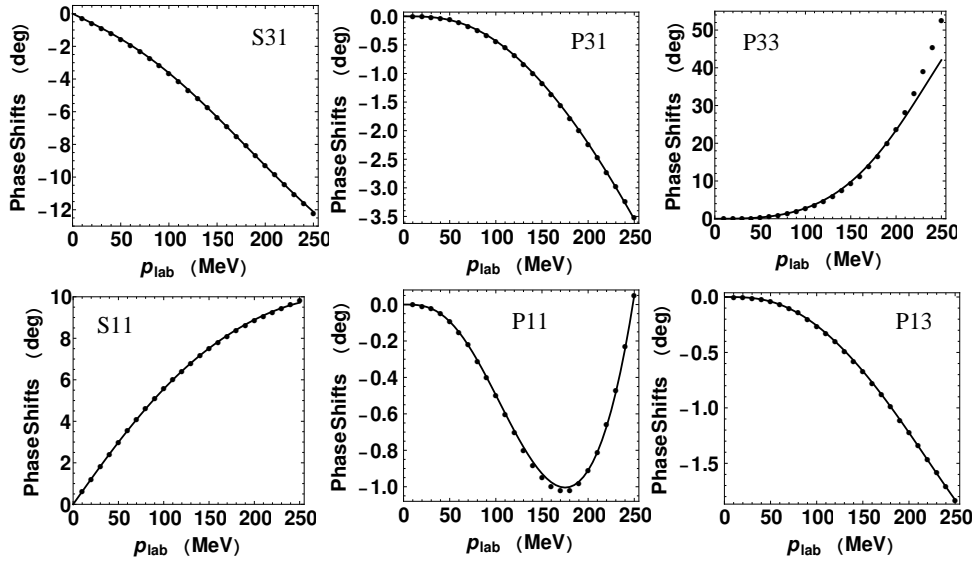


Figure 3: Fits for the WI08 phase shifts versus the pion lab. momentum $|\mathbf{p}_{\text{lab}}|$ in pion-nucleon (πN) scattering at fourth order. Fitting for all πN waves are the data in the range of 50-250 MeV.

SU(3) HB χ PT. We fitted the WI08 phase shifts of πN scattering in range of 50-150 MeV pion lab. momentum to determine the M_0 and the LECs. This led to an excellent description of S - and P -wave phase shifts below 200 MeV pion lab. momentum. The scattering lengths and scattering volumes were also calculated at this order, which turned out to be in good agreement with those of other approaches and available experimental data. We discussed the convergence of the chiral expansion based on the phase shifts and threshold parameters from the best fits up to the respective order in detail. To sum up, we obtained a good convergence in πN scattering at this order. Finally, we extended the description for phase shifts of πN scattering to 250 MeV pion lab. momentum. The reasonable M_0 and LECs are also obtained. They can be used for the other physical processes as input. A good description of all waves except for the $P33$ -wave at high energy were obtained. An improved result for πN scattering may be achieved through including the resonance $\Delta(1232)$ and the other hadronic contributions.

Acknowledgments

This work is supported by the National Natural Science Foundation of China under Grant No. 11947036. I thank Norbert Kaiser (Technische Universität München), Yan-Rui Liu (Shandong University), Li-Sheng Geng (Beihang University), Jun-Xu Lu (Beihang University) and Jing Ou-Yang (Jishou University) for very helpful discussions.

References

- [1] S. Weinberg. Phenomenological Lagrangians. *Physica A*, 96:327–340, 1979.
- [2] J. Gasser and H. Leutwyler. Chiral perturbation theory to one loop. *Annals Phys.*, 158:142, 1984.
- [3] H. Leutwyler. On the foundations of chiral perturbation theory. *Annals Phys.*, 235:165–203, 1994.
- [4] S. Scherer and M. R. Schindler. A primer for chiral perturbation theory. *Lect. Notes Phys.*, 830:pp.1–338, 2012.
- [5] E. E. Jenkins and A. V. Manohar. Baryon chiral perturbation theory using a heavy fermion Lagrangian. *Phys. Lett. B*, 255:558–562, 1991.
- [6] V. Bernard, N. Kaiser, J. Kambor, and U.-G. Meißner. Chiral structure of the nucleon. *Nucl. Phys. B*, 388:315–345, 1992.
- [7] T. Becher and H. Leutwyler. Baryon chiral perturbation theory in manifestly Lorentz invariant form. *Eur. Phys. J. C*, 9:643–671, 1999.

- [8] J. Gegelia and G. Japaridze. Matching heavy particle approach to relativistic theory. *Phys. Rev. D*, 60:114038, 1999.
- [9] T. Fuchs, J. Gegelia, G. Japaridze, and S. Scherer. Renormalization of relativistic baryon chiral perturbation theory and power counting. *Phys. Rev. D*, 68:056005, 2003.
- [10] M. R. Schindler, T. Fuchs, J. Gegelia, and S. Scherer. Axial, induced pseudoscalar, and pion-nucleon form-factors in manifestly Lorentz-invariant chiral perturbation theory. *Phys. Rev. C*, 75:025202, 2007.
- [11] L. S. Geng, J. Martin Camalich, L. Alvarez-Ruso, and M. J. Vicente Vacas. Leading SU(3)-breaking corrections to the baryon magnetic moments in chiral perturbation theory. *Phys. Rev. Lett.*, 101:222002, 2008.
- [12] J. Martin Camalich, L. S. Geng, and M. J. Vicente Vacas. The lowest-lying baryon masses in covariant SU(3)-flavor chiral perturbation theory. *Phys. Rev. D*, 82:074504, 2010.
- [13] X. L. Ren, L. S. Geng, J. Martin Camalich, J. Meng, and H. Toki. Octet baryon masses in next-to-next-to-next-to-leading order covariant baryon chiral perturbation theory. *JHEP*, 12:073, 2012.
- [14] J. M. Alarcón, J. Martin Camalich, and J. A. Oller. The chiral representation of the πN scattering amplitude and the pion-nucleon sigma term. *Phys. Rev. D*, 85:051503, 2012.
- [15] J. M. Alarcón, J. Martin Camalich, and J. A. Oller. Improved description of the πN scattering phenomenology in covariant baryon chiral perturbation theory. *Annals Phys.*, 336:413–461, 2013. [Private communication with J.M. Alarcón].
- [16] L.-S. Geng. Recent developments in SU(3) covariant baryon chiral perturbation theory. *Front. Phys.*, 8:328–348, 2013.
- [17] Y.-H. Chen, D.-L. Yao, and H. Q. Zheng. Analyses of pion-nucleon elastic scattering amplitudes up to $\mathcal{O}(p^4)$ in extended-on-mass-shell subtraction scheme. *Phys. Rev. D*, 87:054019, 2013.
- [18] D.-L. Yao, D. Siemens, V. Bernard, E. Epelbaum, A. M. Gasparyan, J. Gegelia, H. Krebs, and U.-G. Meißner. Pion-nucleon scattering in covariant baryon chiral perturbation theory with explicit Delta resonances. *JHEP*, 05:038, 2016.
- [19] J.-X. Lu, L.-S. Geng, X.-L. Ren, and M.-L. Du. Meson-baryon scattering up to the next-to-next-to-leading order in covariant baryon chiral perturbation theory. *Phys. Rev. D*, 99(5):054024, 2019.
- [20] N. Fettes, U.-G. Meißner, and S. Steininger. Pion-nucleon scattering in chiral perturbation theory (I): Isospin symmetric case. *Nucl. Phys. A*, 640:199–234, 1998.
- [21] N. Fettes and U.-G. Meißner. Pion nucleon scattering in chiral perturbation theory (II): Fourth order calculation. *Nucl. Phys. A*, 676:311, 2000.
- [22] H. Krebs, A. Gasparyan, and E. Epelbaum. Chiral three-nucleon force at N4LO I: Longest-range contributions. *Phys. Rev. C*, 85:054006, 2012.
- [23] D. R. Entem, N. Kaiser, R. Machleidt, and Y. Nosyk. Peripheral nucleon-nucleon scattering at fifth order of chiral perturbation theory. *Phys. Rev. C*, 91(1):014002, 2015.
- [24] M. Hoferichter, J. Ruiz de Elvira, B. Kubis, and U.-G. Meißner. Matching pion-nucleon Roy-Steiner equations to chiral perturbation theory. *Phys. Rev. Lett.*, 115:192301, 2015.
- [25] D. Siemens, J. Ruiz de Elvira, E. Epelbaum, M. Hoferichter, H. Krebs, B. Kubis, and U.-G. Meißner. Reconciling threshold and subthreshold expansions for pion-nucleon scattering. *Phys. Lett. B*, 770:27–34, 2017.
- [26] B.-L. Huang and Y.-D. Li. Kaon-nucleon scattering to one-loop order in heavy baryon chiral perturbation theory. *Phys. Rev. D*, 92(11):114033, 2015. [Erratum: *Phys. Rev. D*95,019903(2017)].
- [27] B.-L. Huang, J.-S. Zhang, Y.-D. Li, and N. Kaiser. Meson-baryon scattering to one-loop order in heavy baryon chiral perturbation theory. *Phys. Rev. D*, 96(11):016021, 2017.
- [28] N. Kaiser. Chiral corrections to kaon nucleon scattering lengths. *Phys. Rev. C*, 64:045204, 2001. [Erratum: *Phys. Rev. C*73,069902(2006)].
- [29] Y.-R. Liu and S.-L. Zhu. Meson-baryon scattering lengths in HB χ PT. *Phys. Rev. D*, 75:034003, 2007.
- [30] Y.-R. Liu and S.-L. Zhu. Decuplet contribution to the meson-baryon scattering lengths. *Eur. Phys. J. C*, 52:177–186, 2007.
- [31] Z.-W. Liu, Y.-R. Liu, and S.-L. Zhu. Pseudoscalar meson and decuplet baryon scattering lengths. *Phys. Rev. D*, 83:034004, 2011.
- [32] Z.-W. Liu and S.-L. Zhu. Pseudoscalar meson and charmed baryon scattering lengths. *Phys. Rev. D*, 86:034009, 2012. [Erratum: *Phys. Rev. D*93,no.1,019901(2016)].

- [33] B.-L. Huang and J. Ou-Yang. Pion-nucleon scattering to $\mathcal{O}(p^3)$ in heavy baryon SU(3) chiral perturbation theory. *Phys. Rev. D*, 101:056021, 2020.
- [34] S.-Z. Jiang, Q.-S. Chen, and Y.-R. Liu. Meson-baryon effective chiral Lagrangians at order p^4 . *Phys. Rev. D*, 95(1):014012, 2017.
- [35] J. Gasser and U.-G. Meißner. On the phase of epsilon-prime. *Phys. Lett. B*, 258:219–224, 1991.
- [36] T. E. O. Ericson and W. Weise. *Pions and nuclei*. Clarendon Press, Oxford, UK, 1988.
- [37] M. Tanabashi *et al.*. Review of Particle Physics. *Phys. Rev. D*, 98(10):030001, 2018.
- [38] C. C. Chang *et al.*. A per-cent-level determination of the nucleon axial coupling from quantum chromodynamics. *Nature*, 558:91–94, 2018.
- [39] B. Märkisch *et al.*. Measurement of the weak axial-vector coupling constant in the decay of free neutrons using a pulsed cold neutron beam. *Phys. Rev. Lett.*, 122:242501, 2019.
- [40] W. J. Briscoe *et al.*, SAID on-line program, see <http://gwdac.phys.gwu.edu>.
- [41] R. L. Workman, R. A. Arndt, W. J. Briscoe, M. W. Paris, and I. I. Strakovsky. Parameterization dependence of T matrix poles and eigenphases from a fit to πN elastic scattering data. *Phys. Rev. C*, 86:035202, 2012.
- [42] J. Dobaczewski, W. Nazarewicz, and P.-G. Reinhard. Error estimates of theoretical models: a Guide. *J. Phys. G*, 41:074001, 2014.
- [43] B. D. Carlsson *et al.*. Uncertainty analysis and order-by-order optimization of chiral nuclear interactions. *Phys. Rev. X*, 6(1):011019, 2016.
- [44] H. C. Schroder *et al.*. The pion nucleon scattering lengths from pionic hydrogen and deuterium. *Eur. Phys. J. C*, 21:473–488, 2001.
- [45] V. Baru, C. Hanhart, M. Hoferichter, B. Kubis, A. Nogga, and D. R. Phillips. Precision calculation of the π^-d scattering length and its impact on threshold πN scattering. *Phys. Lett. B*, 694:473–477, 2011.
- [46] V. Baru, C. Hanhart, M. Hoferichter, B. Kubis, A. Nogga, and D. R. Phillips. Precision calculation of threshold π^-d scattering, πN scattering lengths, and the GMO sum rule. *Nucl. Phys. A*, 872:69–116, 2011.
- [47] M. Hoferichter, V. Baru, C. Hanhart, B. Kubis, A. Nogga, and D. R. Phillips. Isospin breaking in pion deuteron scattering and the pion nucleon scattering lengths. *Proc. Sci.*, CD12:093, 2013.
- [48] M. Hennebach *et al.*. Hadronic shift in pionic hydrogen. *Eur. Phys. J. A*, 50:190, 2014. [Erratum: *Eur. Phys. J.*A55,no.2,24(2019)].
- [49] M. Hoferichter, J. Ruiz de Elvira, B. Kubis, and U.-G. Meißner. High-precision determination of the pion-nucleon σ -term from Roy-Steiner equations. *Phys. Rev. Lett.*, 115:092301, 2015.
- [50] J. Ruiz de Elvira, M. Hoferichter, B. Kubis, and U.-G. Meißner. Extracting the σ -term from low-energy pion-nucleon scattering. *J. Phys. G*, 45(2):024001, 2018.